PHYSICAL REVIEW D **95,** 096007 (2017)

Breathers and nonlinear waves on open vortex filaments in the nonrelativistic Abelian Higgs model

Robert A. Van Gorder*

Mathematical Institute, University of Oxford, Andrew Wiles Building, Radcliffe Observatory Quarter, Woodstock Road, Oxford, OX2 6GG, United Kingdom

(Received 11 January 2017; published 22 May 2017)

We demonstrate the existence of various nonlinear waves along open vortex filaments in the nonrelativistic Abelian Higgs model. These include nonlinear waves, which give the birth and death of helical filaments, as well breathers, which modify the amplitude of helical filaments periodically in time. Importantly, we demonstrate that some of the dynamics are quite particular to the equation of motion for vortex filaments under the nonrelativistic Abelian Higgs model, giving rise to vortex filament solutions not possible under the hydrodynamic vortex filament equation of motion (the local induction approximation) or generalizations used to study the dynamics of quantized vortex filaments in He^4.

DOI: 10.1103/PhysRevD.95.096007

I. INTRODUCTION

Vortex solutions appear in a wide variety of field-theoretic models, with applications including quantized vortex filaments in He^4 [1], Abrikosov lines in type-II superconductors [2], vortices in Bose-Einstein condensates [3], and cosmic strings [4]. Regarding the latter application, a relativistic form of the Abelian Higgs model which results in Nambu-Goto action [5] gives one model with which to study cosmic string dynamics [6]. Another interesting case is that of the nonrelativistic Abelian Higgs model, which also permits vortex filament solutions [7].

Under the nonrelativistic Abelian Higgs model, the equation of motion under the assumption of negligible dissipation was considered in Ref. [7]. Later, this was generalized to account for the situation in which the gauge field is coupled to the asymmetric background of chiral fermions, in both static [8] and dynamic (time-dependent) [9] cases. The resulting equations of motion can be seen as one possible generalization of the Betchov-Da Rios equations [often referred to as the local induction approximation (LIA)] governing the self-induced motion of a thin vortex filament in hydrodynamics and in particular differ from the generalization used in the study of He^4 which involves mutual friction with a normal fluid flow [10]. While much effort has been spent on understanding vortex filament dynamics in hydrodynamics under the LIA and also for the generalizations to He^4, there are relatively few solutions studied under models such as the nonrelativistic Abelian Higgs model. It is known that in certain limits, helix solutions are possible [8], while in a fairly restrictive limit, the equation of motion is equivalent to the LIA [9] (with helices, rings, and line filaments among those solutions possible).

In the present paper, we demonstrate the existence of more general helixlike vortex filament solutions which depend nonlinearly on time. These include a family of solutions which asymptotically behaves like a line filament for time tending to $\pm\infty$ yet a helix for finite time. This solution allows for a helical filament to come into existence, amplify, and then eventually decay to a line filament. Another interesting solution is a breather filament, which takes the form of a helical filament which has a periodic amplitude in time. Such a solution exhibits the creation and destruction of a helical filament in finite time. We compare these solutions to solutions obtained for similar equations of motion governing vortex filament motion in He^4, demonstrating that some of these solutions differ from known solutions under LIA and generalizations to He^4.

II. VORTEX DYNAMICS UNDER THE NONRELATIVISTIC ABELIAN HIGGS MODEL

We briefly review the derivation in Refs. [7,9]. The action of the nonrelativistic Abelian Higgs model which incorporates gauge vortices can be given in terms of the Lagrangian density acting on the scalar field ψ given by [9]

$$\begin{aligned}\mathcal{L} = {} & \frac{1}{8\pi}\left(\left(-\partial_\tau \frac{\mathbf{A}}{c} - \nabla\varphi\right)^2 - (\nabla\times\mathbf{A})^2\right) - \frac{g}{2}(|\psi|^2 - n_0)^2 \\ & + \frac{1}{2}\{\psi^*(i\hbar\partial_\tau - q(\varphi - a_0)) + \psi(i\hbar\partial_\tau - q(\varphi - a_0))^*\} \\ & - \frac{1}{2m}\left|\left(-i\hbar\nabla - \frac{q}{c}(\mathbf{A} - \mathbf{a})\right)\psi\right|^2 - \rho_0\varphi, \end{aligned} \tag{1}$$

where $A_\mu = (\varphi, \mathbf{A})$ is the 4-vector gauge potential; ∂_τ is the time partial derivative; q and m are the charge and mass of particles forming the condensate of the scalar field ψ; n_0 is the density of the scalar field condensation; ρ_0 is the homogeneous positive charge density, selected to give net

*Robert.VanGorder@maths.ox.ac.uk

neutrality of the system ($\rho_0 + qn_0 = 0$); g is a coupling constant; $\hbar$ is the reduced Planck constant; and c is the speed of light.

Before going on, a comment about how this Lagrangian was derived is in order, since we do not reproduce a derivation here. This Lagrangian was developed in Ref. [7] to study the dynamics of the curved line defects based on field-theoretic models and to scrutinize the role of the excitations of the gauge and scalar fields exchanged between the different segments of the vortex. Local (gauge) vortex equations of motion were obtained from the effective action of the Abelian Higgs model at zero temperature. The same task is performed for the global vortex by taking the limit of the vanishing gauge coupling constant. This framework includes the background contribution, which is essential for the static situation, in addition to the excitations. A fully three-dimensional geometry is considered. The expressions for the transverse Magnus-like force and the effective masses of the local and global vortices are obtained.

The vortex is represented as the curve of singular phase χ_s of the scalar field $\psi = \sqrt{n_0}\exp(i\chi_s)$ which forms the spatially homogeneous condensate of the density n_0 everywhere except for the vortex core, where it goes to zero at the transverse distances of the order of the healing (or correlation) length ξ. With this, the vector $a_\mu = (a_0, \mathbf{a}) = -\frac{\hbar c}{q}\partial_\mu \chi_s$ is the 4-gradient of the singular phase,

$$[\nabla \times \nabla]\chi_s = 2\pi \int d\sigma \mathbf{X}' \delta^{(3)}(\mathbf{x} - \mathbf{X}), \tag{2}$$

serving as the source of the gauge vortex with the unit flux quantum of which the space-time location is given by the vector $\mathbf{X}$. Taking $\mathbf{X}(\tau, \sigma)$ to denote the vortex filament curve (σ is the arclength along the curve, while τ denotes time), we may obtain [9] the components of a_μ (in the gauge $\nabla \mathbf{a} = 0$),

$$a_0 = \frac{\hbar}{2q}\oint_\ell \frac{(\mathbf{X}_\tau(\tau,\sigma) \times \mathbf{X}_\sigma(\tau,\sigma)) \cdot (\mathbf{x}(\tau,\hat{\sigma}) - \mathbf{X}(\tau,\sigma))}{|\mathbf{x}(\tau,\hat{\sigma}) - \mathbf{X}(\tau,\sigma)|^3} d\hat{\sigma}, \tag{3}$$

$$\mathbf{a} = \frac{\hbar c}{2q}\oint_\ell \frac{\mathbf{X}_\sigma(\tau,\sigma) \times (\mathbf{x}(\tau,\hat{\sigma}) - \mathbf{X}(\tau,\sigma))}{|\mathbf{x}(\tau,\hat{\sigma}) - \mathbf{X}(\tau,\sigma)|^3} d\hat{\sigma}. \tag{4}$$

The equation of motion of the gauge vortex filament resulting from the Lagrangian density given in (1) is shown to be [7,9]

$$\frac{1}{c_0^2}\mathbf{X}_{\tau\tau} - \mathbf{X}_{\sigma\sigma} + \frac{1}{\gamma}[\mathbf{X}_\tau \times \mathbf{X}_\sigma] + \frac{\tilde{\mu}}{\gamma}[\mathbf{X}_\sigma \times \mathbf{X}_{\sigma\sigma\sigma}], \tag{5}$$

where

$$\gamma = \frac{\hbar}{2m}\ln\left(\frac{\lambda_L}{\xi}\right), \qquad T_0 = \frac{\hbar}{2mc_s^2}\ln\left(\frac{\lambda_s}{\xi}\right),$$
$$\tilde{\mu} = \frac{\mu_f}{4\pi^2\hbar n_0}, \qquad c_0 = \sqrt{\frac{\gamma}{T_0}} = c_s\sqrt{\frac{\ln(\lambda_L/\xi)}{\ln(\lambda_s/\xi)}}. \tag{6}$$

Here,

$$\lambda_L = \sqrt{\frac{mc^2}{4\pi n_0 q^2}}, \quad c_s = \sqrt{\frac{n_0 g}{m}}, \quad \xi = \frac{\hbar}{2mc_s} \tag{7}$$

are the London penetration depth, the velocity of sound, and the healing length (the characteristic size of the vortex core), respectively; μ_f is the chemical potential; and the intermediate scale $\lambda_s = \lambda_L c_s/c \ll \lambda_L$. It was pointed out [8] that in the limit $T_0 = 0$ and $\tilde{\mu} \neq 0$ a nontrivial static solution is found in the form of a helical filament. Note also that in the limit $T_0 = 0$ and $\tilde{\mu} = 0$ one would have recovered $\mathbf{X}_t = \gamma\kappa\mathbf{b}$ (where κ is the curvature and $\mathbf{b}$ is the binormal vector), which is the LIA for the self-induced motion of vortex filaments.

Usually, while deriving the equation of motion for the center line of the vortex from the dynamics of an underlying field, one assumes that the radius of curvature of the filament curve is much larger than the core size, as previously discussed for hydrodynamic fields and vortex filaments [11–14]. Mathematically, the filament curve described by $\mathbf{X}(\tau, \sigma)$ should therefore be of sufficient bounded variation. That is to say, the filament should not change too rapidly over space [15]. In the purely helical case, this means that the product of amplitude and wave number, Ak, should be sufficiently bounded. Otherwise, for large Ak, the assumptions in the local approximation break down. For a discussion of the breakdown for rapidly varying vortex filaments via a comparison with local (LIA) and nonlocal (Biot-Savart) models, see Ref. [16].

A. Nondimensional vortex filament equation

Since we shall be interested in the $T_0 > 0, \tilde{\mu} > 0$ regime, let us introduce the nondimensionalization

$$\mathbf{X}(\tau, \sigma) = r_0 \mathbf{r}(t, s), \tag{8}$$

where

$$r_0 = \sqrt{\gamma T_0}, \qquad s = s_0\sigma = \sqrt{\frac{c_0}{\tilde{\mu}}}\sigma, \qquad t = t_0\tau = \sqrt{\frac{c_0^3}{\tilde{\mu}}}\tau, \tag{9}$$

which puts Eq. (5) into the form of the vector nonlinear wave equation

$$\mathbf{r}_{tt} - \mathbf{r}_{ss} + \mathbf{r}_t \times \mathbf{r}_s + \mathbf{r}_s \times \mathbf{r}_{sss} = \mathbf{0}. \tag{10}$$

This form of the vortex filament equation will make the following analysis more tractable.

B. Scalar PDE system

Note that a solution $\mathbf{r}(t,s)$ to Eq. (10) can be written in terms of three real-valued functions,

$$\mathbf{r}(t,s) = [\Phi(t,s), Y(t,s), Z(t,s)]^T. \tag{11}$$

Placing this into Eq. (10), we obtain the partial differential equation (PDE) system

$$\Phi_{tt} - \Phi_{ss} + Y_t Z_s - Y_s Z_t + Y_s Z_{sss} - Y_{sss} Z_s = 0, \tag{12}$$

$$Y_{tt} - Y_{ss} + \Phi_s Z_t - \Phi_t Z_s + \Phi_{sss} Z_s - \Phi_s Z_{sss} = 0, \tag{13}$$

$$Z_{tt} - Z_{ss} - \Phi_s Y_t + \Phi_t Y_s - \Phi_{sss} Y_s + \Phi_s Y_{sss} = 0. \tag{14}$$

Often, one assumes the length of a vortex filament is aligned roughly along one axis, with the components along the other axis measuring deflections from this central axis. Let us assume that the vortex filament is aligned along the first component in Eq. (11). Further, by symmetry present in the system (12)–(14), we define $\Psi(t,s) = Y(t,s) + iZ(t,s)$. Then, adding Eq. (13) to i times Eq. (14), one obtains a single equation for Ψ, and we obtain the system of nonlinear wave equations

$$\Phi_{tt} - \Phi_{ss} - \frac{i}{4}\{\Psi_s \Psi_t^* - \Psi_s^* \Psi_t + \Psi_s^* \Psi_{sss} - \Psi_s \Psi_{sss}^*\} = 0, \tag{15}$$

$$\Psi_{tt} - \Psi_{ss} + i\{\Phi_t \Psi_s - \Phi_s \Psi_t + \Phi_s \Psi_{sss} - \Phi_{sss} \Psi_s\} = 0, \tag{16}$$

for real-valued field Φ and complex-valued field Ψ. This system is the analog of similar nonlinear Schrödinger (NLS) equations for classical vortex filaments or vortex filaments in He^4.

III. VORTEX FILAMENT SOLUTIONS

From our understanding of vortex solutions under LIA in He^4, we expect that a thin vortex may have waves or perturbations which undergo translation, rotation, and amplification along a central axis. Therefore, it makes sense to consider a family of particular solutions of the form

$$\mathbf{r}(t,s) = [s - \beta(t), A(t)\cos(ks - \omega(t)), A(t)\sin(ks - \omega(t))]^T. \tag{17}$$

The function β denotes translational motion, ω gives rotational motion, and changes in A give the amplification or decay of waves along the vortex. When $A = 0$, we have a line vortex, while when $A \neq 0$, we have a wavy (helical) vortex solution. Such waves along a line filament are often referred to as Kelvin waves. When $A \neq 0$ is constant, we have a purely helical solution, and the amplitude of the Kelvin waves will not change with time. The parameter k is the wave number, and this will determine how tightly coiled the vortex solution is. Note that this solution ansatz (17) is equivalent to taking the ansatz $\Phi(t,s) = s - \beta(t)$ and $\Psi(t,s) = A(t)\exp(i\{ks - \omega(t)\})$ in Eqs. (15) and (16).

Placing the assumed solution (17) into Eq. (10), we obtain

$$\begin{bmatrix} kA\dot{A} - \ddot{\beta} \\ (2\dot{\omega}+1)\dot{A}\sin(ks-\omega(t)) + \mathcal{M}\cos(ks-\omega(t)) \\ -(2\dot{\omega}+1)\dot{A}\cos(ks-\omega(t)) + \mathcal{M}\sin(ks-\omega(t)) \end{bmatrix} = \mathbf{0}, \tag{18}$$

where $\mathcal{M} = \ddot{A} + [k^3 - k^2 - \dot{\omega} - \dot{\omega}^2 + k\dot{\beta}]A$. This puts a restriction on the possible forms of β, ω, and A and is equivalent to the system of ordinary differential equations

$$kA\dot{A} - \ddot{\beta} = 0, \tag{19}$$

$$(2\dot{\omega}+1)\dot{A} = 0, \tag{20}$$

$$\ddot{A} + (k^3 - k^2 - \dot{\omega} - \dot{\omega}^2 + k\dot{\beta})A = 0. \tag{21}$$

A solution to Eqs. (19)–(21) will then provide us with a vortex solution (17).

A. Kelvin waves along filaments

In the case in which $A(t) = A_0$, a constant, Eqs. (19)–(21) imply that $\beta(t) = \beta_1 t + \beta_0$ and $\omega(t) = \omega_1 t + \omega_0$, provided that the constants β_1 and ω_1 satisfy the algebraic condition

$$-\omega_1^2 - \omega_1 + k\beta_1 + k^3 - k^2 = 0. \tag{22}$$

This is the condition for a regular helical solution. For $k \neq 0$ and arbitrary rotational velocity ω_1, Kelvin waves along the vortex filament translate with translational velocity,

$$\beta_1 = \frac{\omega_1(\omega_1+1) + k^2(1-k)}{k}. \tag{23}$$

The vortex filament solution in this case is given by

$$\mathbf{r}(t,s) = \begin{bmatrix} s - \frac{\omega_1(\omega_1+1)+k^2(1-k)}{k}t - \beta_0 \\ A_0\cos(ks - \omega_1 t - \omega_0) \\ A_0\sin(ks - \omega_1 t - \omega_0) \end{bmatrix}. \tag{24}$$

As waves on the vortex filament rotate more rapidly, the rate of translation of the Kelvin waves along the filament

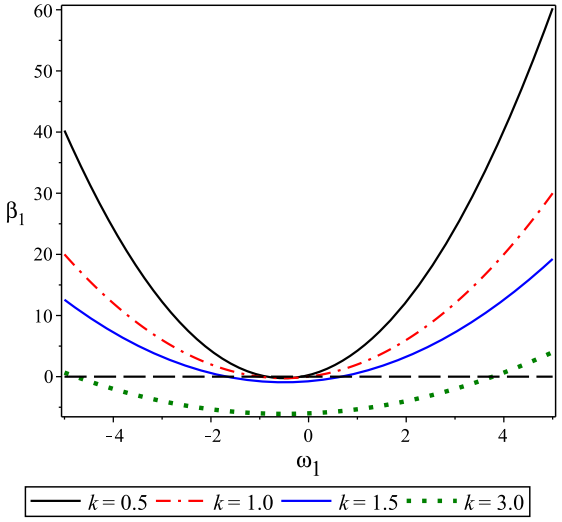

FIG. 1. Plot of the Kelvin wave translational velocity β_1 as a function of the rotational velocity ω_1, for various fixed values of wave number k.

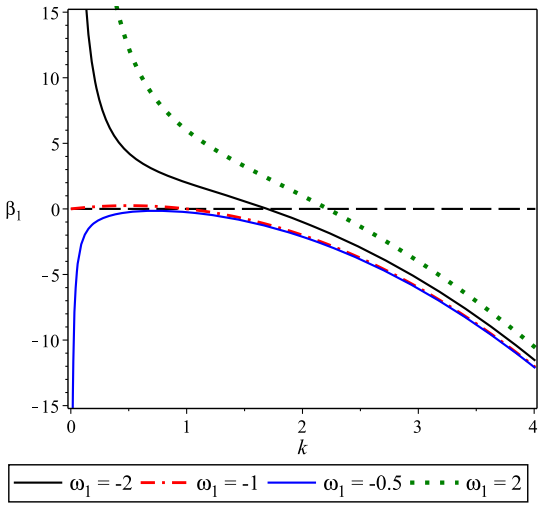

FIG. 2. Plot of the Kelvin wave translational velocity β_1 as a function of the wave number k, for various fixed values of the rotational velocity ω_1.

increases (for fixed k). The influence of k is perhaps more interesting. As k increases (corresponding to more tightly coiled solutions), there will be a reversal in the direction of propagation of the Kelvin waves. Indeed, for $\omega_1 > 0$, the wave will propagate toward increasing arclength $s \to \infty$ for a large time if $k > 0$ is small, while the wave will propagate toward negative arclength (in the opposite direction along the filament, as toward $s \to -\infty$) for large $k > 0$. The critical value between these two corresponds to the positive root of $\omega_1(\omega_1 + 1) + k^2(1 - k)$. When $\omega_1 < 0$ (the rotation corresponds to the counterflow case), the situation is more complicated, with two positive critical values of k for which there is a change in the direction of propagation of the Kelvin waves. In Fig. 1, we plot the translational velocity of Kelvin waves as a function of the angular velocity, while in Fig. 2, we plot the translational velocity as a function of the wave number.

One may show that these are the only traveling waves which move along a filament. One can search for another class of traveling wave solutions which are not aligned along a central axis. The most general such solutions would take the form $\mathbf{r}(s,t) = \mathbf{R}(ks - \eta t)$. From the form of Eq. (10), we should have a bounded solution in the wave variable $s - t$ and an unbounded solution in the wave variable $s + t$. The bounded wave solution then takes the form

$$\mathbf{r}(t,s) = \mathbf{C}^{[0]} + \mathbf{C}^{[1]}\cos(s-t) + \mathbf{C}^{[2]}\sin(s-t), \quad (25)$$

where $\mathbf{C}^{[j]} \in \mathbb{R}^3$ is a constant vector for $j = 0, 1, 2$.

More generally, for the wave variable $z = ks - \eta t$, we consider

$$\mathbf{r}(s,t) = [s + \beta(z), f(z), g(z)]^T. \quad (26)$$

Such waves are disturbances along a line filament $[s, 0, 0]^T$ which propagates in the $\pm s$ direction (depending on the sign of η). From Eq. (10), we obtain the system

$$(\eta^2 - k^2)\beta'' + k^4(f'g''' - g'f''') = 0, \quad (27)$$

$$(\eta^2 - k^2)f'' - \eta g' - k^3 g''' + k^4(g'\beta''' - \beta' g''') = 0, \quad (28)$$

$$(\eta^2 - k^2)g'' + \eta f' + k^3 f''' - k^4(f'\beta''' - \beta' f''') = 0. \quad (29)$$

This system is in general singular yet admits a solution when each unknown function takes the form $C_0 + C_1\exp(\Omega z)$. When Ω is purely imaginary, we can recover the helical filaments. When $\mathrm{Re}[\Omega] \neq 0$, then there is unbounded growth for one of the limits $s \to \pm\infty$, and so the filament becomes unbounded away from the reference axis.

B. Creation and destruction of Kelvin waves

If A is not constant, then by Eq. (20), we must have $\omega(t) = \omega_0 - t/2$. Similarly, by Eq. (19), we need $\dot{\beta} = \beta_1 + \frac{k}{2}A^2$. Placing these into Eq. (21), we obtain a single equation for A; to wit,

$$\ddot{A} + \left(k^3 - k^2 + \beta_1 k + \frac{1}{4}\right)A + \frac{k^2}{2}A^3 = 0. \quad (30)$$

When $k > 0$ and $\beta_1 < \beta_1^*(k) = k - k^2 - (4k)^{-1}$, Eq. (30) has the exact solution

$$A(t) = \frac{2}{k}\hat{A}_1(t), \quad (31)$$

where

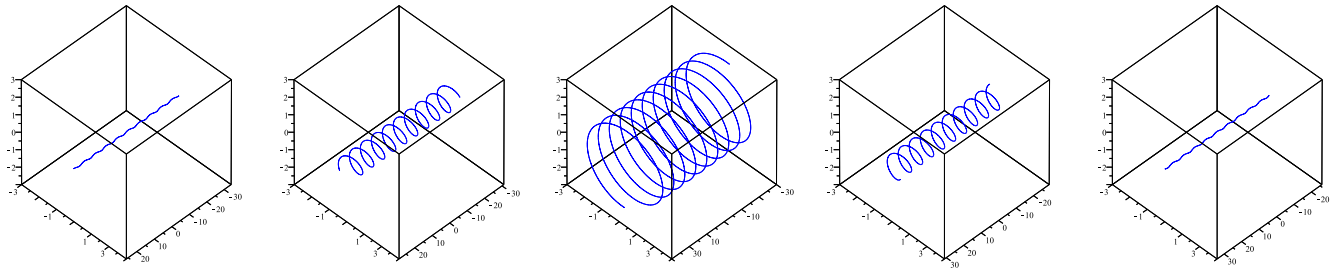

FIG. 3. Plot of the growth and decay of a helical vortex filament under the solution representation (33) for $k = 1, \beta_1 = -1, \beta_0 = 0$, and $\omega_0 = 0$. Time values taken are (left to right) $t = -5, -2, 0, 2, 5$.

$$\hat{A}_1(t) = \sqrt{k(\beta_1^*(k) - \beta_1)}\,\mathrm{sech}\left(\sqrt{k(\beta_1^*(k) - \beta_1)}t\right). \tag{32}$$

This results in the vortex filament solution

$$\mathbf{r}(t,s) = \begin{bmatrix} s - \beta_1 t - \beta_0 - \int_0^t (\hat{A}_1(q))^2 dq \\ \frac{2}{k}\hat{A}_1(t)\cos(ks + t/2 - \omega_0) \\ \frac{2}{k}\hat{A}_1(t)\sin(ks + t/2 - \omega_0) \end{bmatrix}. \tag{33}$$

As $t \to \pm\infty$, this solution behaves like a straight line filament, while for finite t, the solution behaves like a helical filament. The maximal amplitude is attained at $t = 0$. This solution therefore models the creation and dissipation of Kelvin waves along the vortex filament. Note that for the present case the maximal translational velocity of waves along the filament corresponds to the maximum amplitude of the waves. In Fig. 3, we plot the filament solution (33) for various values of time, showing the creation of a helix from a perturbed line filament and then the decay of this filament structure.

Note that the creation and decay are not observed in the LIA or Biot-Savart model for the motion of a vortex filament in He^4. In that case, one either has amplification or decay, but not both, for a single solution. Runaway amplification of the analytical solutions corresponds to the Donnelly-Glaberson instability seen experimentally and numerically [17–20]. For the nonrelativistic Abelian Higgs model, runaway amplification does not appear to occur, with an amplifying filament instead decaying after it amplifies to the maximum possible extent away from the center axis of the filament. This highlights one important way these vortex filament solutions differ from those found for other models.

C. Breathers along vortex filaments

While we have so far demonstrated the existence of constant amplitude and sech(t)-type amplitude solutions, corresponding to an eternal helical filament and the formation and dissipation of a helical filament, respectively, it remains to be shown that there are breather-type solutions. Such solutions would exhibit pulselike behavior in time. Noting that for some parameter values Eq. (30) should have Jacobi elliptic function solutions, we find that there exists a class of solutions parametrized by amplitude $a > 0$ given by

$$A(t) = a\hat{A}_2(t), \tag{34}$$

where

$$\hat{A}_2(t) = \mathrm{cn}\left(\frac{\kappa t}{2}, \frac{ak}{\kappa}\right) \tag{35}$$

and

$$\kappa = \sqrt{1 + 4\beta_1 k + (2a^2 - 4)k^2 + 4k^3}. \tag{36}$$

Here, cn denotes the relevant Jacobi elliptic function. Such solutions exist provided that $\kappa^2 > 0$; i.e., κ must be real valued. We therefore have the solution

$$\mathbf{r}(t,s) = \begin{bmatrix} s - \beta_1 t - \beta_0 - \frac{a^2 k}{2}\int_0^t (\hat{A}_2(q))^2 dq \\ a\hat{A}_2(t)\cos(ks + t/2 - \omega_0) \\ a\hat{A}_2(t)\sin(ks + t/2 - \omega_0) \end{bmatrix}. \tag{37}$$

This solution represents a breather; a representative solution is shown in Fig. 4. Indeed, at $t = 0$, we have a helical vortex filament with amplitude a. As time increases, this solution decreases in amplitude to a line filament, then increases in amplitude with the reverse twist direction, decreases in amplitude to a line filament again, and finally increases in amplitude with the original twist orientation. This process continues over each period of the Jacobi elliptic function cn.

These breather solutions feature amplitude as an arbitrary parameter, a, while the solution (33) has amplitude fixed in a relationship depending on the helix wave number k. Therefore, the solution giving growth for $t < 0$ and decay for $t > 0$ is really a rather special case, while the breather solution we exhibit in Eq. (37) is far more ubiquitous in parameter space.

Note that there are no single-twist reversing solutions (solutions which reverse the twist and keep it under the new

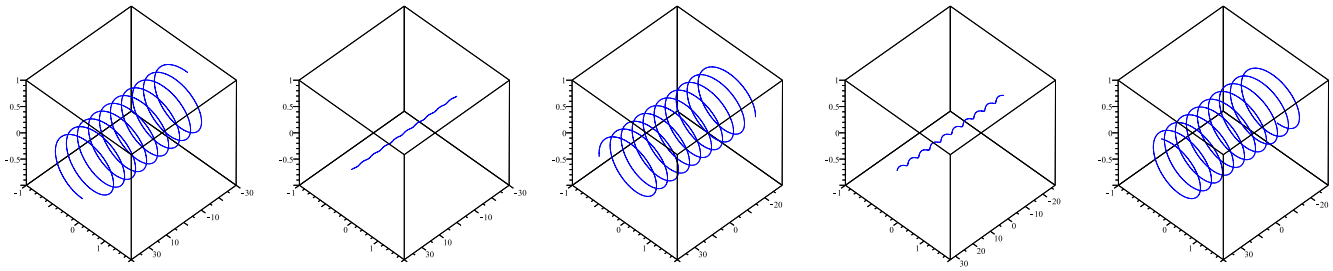

FIG. 4. Plot of the breather vortex filament under the solution representation (37) for $k = 1$, $a = 1/2$, $\beta_1 = -1/8$, $\beta_0 = 0$, and $\omega_0 = 0$. Time values taken are (left to right) $t = 0$, 3.2, 6.4, 10.0, 13.4.

orientation indefinitely). Such a solution would correspond to $A(t) \sim \tanh(t)$, which is not possible for real-valued wave number k.

IV. DISCUSSION

We have demonstrated the existence of breathers and other nonlinear waves along open vortex filaments in the nonrelativistic Abelian Higgs model. All of these solutions are generalizations of helical vortex filaments, and hence waves along these filaments are essentially generalized Kelvin waves with time-varying amplitude. Although the equation of motion shares some characteristics of equations governing the dynamics of hydrodynamic vortex filaments, the solutions we obtain are qualitatively quite distinct from the vortex filament solutions found, say, in the study of quantized vortex filaments in He^4.

Amplifying solutions for the nonrelativistic Abelian Higgs model reach a maximal deflection away from a centrally defined axis and then deamplify. Solutions of this type of equation will amplify and then decay once (giving rise to a helical vortex filament for intermediate times) or amplify/decay periodically (giving rise to breathers along the vortex filament). This behavior is fundamentally different from quantized vortex filaments in He^4, which can either (i) amplify and then destabilize, (ii) maintain fixed amplitude in time, or (iii) decay into line filaments. This process is referred to as the Donnelly-Glaberson instability [17–19] and is observed in both the quantum form of the LIA [21] and the nonlocal Biot-Savart dynamics [20]. While i above is sometimes mentioned as a possible route to quantum turbulence, note that there is disagreement about this. Kelvin waves, by definition, are a small perturbation of the vortex filaments, and their dynamics is a very small part of the overall dynamics of vortex tangle. Only a full-scale deformation may lead to a collision (or self-collision) of vortex filaments and then to reconnection and development of chaos. See details of this discussion in the review [22]. Still, the amplification of such quantized vortex filaments within the quantum form of the LIA can be undesirable, as if the filament amplifies too far, it may violate the bounded variation requirement, and hence the assumptions of a local model. While it shares some similarities with the equation of motion for the quantized LIA, the equation of motion for vortex filaments under the nonrelativistic Abelian Higgs model permits solutions which self-regulate to avoid this manner of amplification leading to blowup. Such a solution shares some similarities with the Peregrine soliton [23–25], which is a type of NLS water wave solution which amplifies and then decays back to the ground start. Because of this attribute, the Peregrine soliton has been suggested as a model of rogue waves [24,25]. The solution we obtain is simpler, only involving space in the phase, resulting in a temporal scaling of a helical filament.

Breather structures were found for the LIA and in simulations for quantized vortex filaments [26]. These breathers are NLS breathers which, by way of the Hasimoto transformation [27], are mapped into homoclinic vortex filament solutions [28]. However, these breathers differ from ones we have found here for the nonrelativistic Abelian Higgs model. The LIA breathers can eventually evolve so that distinct segments of the vortex filament interact in finite time, leading to vortex ring shedding as seen in the simulations of Ref. [26]. In contrast, the breather solutions we obtain for the nonrelativistic Abelian Higgs model result in a type of pulsating behavior of Kelvin waves along the vortex filament, and such filaments will always maintain their structure. These differences point to the fact that we have obtained a breather solution which is fundamentally different than the breathers obtained in hydrodynamic models, such as the NLS breather [29] and also the sine-Gordon breather [30]. Indeed, the breather solution we obtain is markedly simpler than the aforementioned breather solutions from the literature.

Note that self-similar solutions do not exist, which is one qualitative difference between Eq. (5) and the local induction approximation for classical [31] and quantized [32,33] vortex filaments. One may also verify that planar filaments will not exist in this model, either, which is what we see for the generalized LIA, which includes mutual friction contributions [34]. This is in contrast to the classical LIA, which does permit such solutions [35].

[1] S. K. Nemirovskii and W. Fiszdon, Rev. Mod. Phys. **67**, 37 (1995).
[2] A. A. Abrikosov, Zh. Eksp. Theor. Fiz. **32**, 1442 (1957).
[3] K. W. Madison, F. Chavy, W. Wohlleben, and J. Dalibard, Phys. Rev. Lett. **84**, 806 (2000).
[4] A. Vilenkin and E. P. S. Shellard, *Cosmic Strings and Other Topological Defects* (Cambridge University Press, Cambridge, England, 1994).
[5] J. Scherk, Rev. Mod. Phys. **47**, 123 (1975).
[6] D. Förster, Nucl. Phys. **B81**, 84 (1974).
[7] A. A. Kozhevnikov, Int. J. Mod. Phys. B **24**, 605 (2010).
[8] A. A. Kozhevnikov, Phys. Lett. B **461**, 256 (1999).
[9] A. A. Kozhevnikov, Phys. Lett. B **750**, 122 (2015).
[10] K. W. Schwarz, Phys. Rev. B **31**, 5782 (1985).
[11] L. M. Pismen, *Vortices in Nonlinear Fields* (Clarendon, Oxford, 1999).
[12] K. Lee, arXiv:cond-mat/9409046.
[13] O. Törnkvist and E. Schröder, Phys. Rev. Lett. **78**, 1908 (1997).
[14] S. K. Nemirovskii, Theor. Math. Phys. **141**, 1452 (2004).
[15] R. A. Van Gorder, Phys. Rev. E **93**, 052208 (2016).
[16] R. A. Van Gorder, J. Fluid Mech. **762**, 141 (2015).
[17] D. K. Cheng, W. M. Cromar, and R. J. Donnelly, Phys. Rev. Lett. **31**, 433 (1973).
[18] W. I. Glaberson, W. W. Johnson, and R. M. Ostermeier, Phys. Rev. Lett. **33**, 1197 (1974).
[19] R. M. Ostermeier and W. I. Glaberson, J. Low Temp. Phys. **21**, 191 (1975).
[20] R. A. Van Gorder, Proc. R. Soc. A **471**, 20150149 (2015).
[21] R. A. Van Gorder, Phys. Fluids **26**, 075101 (2014).
[22] S. K. Nemirovskii, Phys. Rep. **524**, 85 (2013).
[23] D. H. Peregrine, J. Aust. Math. Soc. Series B, Appl. Math. **25**, 16 (1983).
[24] B. Kibler, J. Fatome, C. Finot, G. Millot, F. Dias, G. Genty, N. Akhmediev, and J. M. Dudley, Nat. Phys. **6**, 790 (2010).
[25] R. A. Van Gorder, J. Phys. Soc. Jpn. **83**, 054005 (2014).
[26] H. Salman, Phys. Rev. Lett. **111**, 165301 (2013).
[27] H. Hasimoto, J. Fluid Mech. **51**, 477 (1972).
[28] M. Umeki, Theor. Comput. Fluid Dyn. **24**, 383 (2010).
[29] N. N. Akhmediev, V. M. Eleonskii, and N. E. Kulagin, Theor. Math. Phys. **72**, 809 (1987).
[30] M. J. Ablowitz, D. J. Kaup, A. C. Newell, and H. Segur, Phys. Rev. Lett. **30**, 1262 (1973).
[31] R. A. Van Gorder, J. Fluid Mech. **802**, 760 (2016).
[32] T. Lipniacki, J. Fluid Mech. **477**, 321 (2003).
[33] T. Lipniacki, Phys. Fluids **15**, 1381 (2003).
[34] R. A. Van Gorder, Proc. R. Soc. A **470**, 20140341 (2014).
[35] H. Hasimoto, J. Phys. Soc. Jpn. **31**, 293 (1971).